STUDY ON MEASUREMENT AND PREDICTION METHODS OF NONLINEAR THERMAL CONDUCTIVITY OF HIGH-TEMPERATURE RESISTANT POROUS INSULATION

Xuanyi AN[1], Xia ZHANG[2], Yufei CAI[3], Cong LIU[4], Zongwei ZHANG[*]

[1] College of Aeronautical Engineering, Civil Aviation University of China, Tianjin 300300, China

[2] Shanghai Academy of Spaceflight Technology, China Aerospace Science and Technology Corporation, Shanghai 201109, China.

3 Xiaomi Communication Technology Co., Ltd, Shenzhen 518000, China.

[4] College of Air Traffic Management, Civil Aviation University of China, Tianjin 300300, China.

[*] College of Aeronautical Engineering, Civil Aviation University of China, Tianjin 300300, China, Corresponding Author, E-mail: zhangzw@cauc.edu.cn

High-temperature insulation materials are critical components of thermal protection systems for hypersonic vehicles, gas turbines, and other advanced technologies. In these contexts, the assessment of thermal insulation performance through the measurement of thermal conductivity is essential. This study measures the effective thermal conductivity of high-dimensional S blanket, aluminum silicate cotton needle felt, and nano-aerogel blanket insulation fibers using the heat flux meter method under two environmental conditions: dry and 60% relative humidity. The experiments covered hot surface temperatures ranging from 50°C to 550°C, encompassing 90 distinct operational conditions. The results elucidate the variation patterns of both the effective and true thermal conductivity of these materials. The findings indicate that (1) fitting models for the effective thermal conductivity of the high-dimensional S blanket, aluminum silicate cotton needle felt, and nano-aerogel blanket provided accurate predictions; (2) Humidity significantly affected both the effective and true thermal conductivity at high temperatures for the high-dimensional S blanket and aluminum silicate cotton needle felt, but had a relatively minor impact on the nano-aerogel blanket.; (3) Incorporating true thermal conductivity allowed for accurate predictions of material performance in 42 experimental conditions, with strong agreement between calculated values and experimental data.

Key words*: Effective thermal conductivity True thermal conductivity Heat flow meter method Least squares fitting, Thermal insulation materials*

1. Introduction

Advancements in aero-engines and hypersonic vehicles have made high temperatures a significant challenge for further progress in these fields. When traveling at hypersonic speeds, aerodynamic heating from the viscous effects of surrounding thin gas sharply raises the surface temperature of the aircraft, especially at the nose tip[1]. However, the precision electronic instruments in the cabin have stringent upper temperature limits. Consequently, the installation of thermal insulation materials capable of withstanding high temperatures is crucial for ensuring the reliable operation of interior equipment[2].

Thermal insulation materials are designed to greatly reduce heat flux. Thermal conductivity is one of the key parameters that reflect the insulating properties of thermal insulation materials, serving as a primary indicator of their quality. Heat transfer in high-porosity thermal insulating materials involves a combination of radiation and thermal conductivity. In porous media, convective heat transfer is negligible if the pore size is less than 4 mm[3]. In fibrous insulation materials with densities of 20 kg/m^3 or more, natural convection is also negligible[4, 5]. While natural convection is often neglected, Verchoor and Greebler identified it as a key factor behind discrepancies between experimental and theoretical heat transfer results in high-porosity materials[6]. The materials investigated in this study demonstrate various heat transfer mechanisms, including conduction, convection, and radiation.

The two commonly used methods for measuring thermal conductivity are the transient method and the steady-state method. Gaosheng Wei, Yusong Liu, and colleagues investigated the thermal conductivity of silica aerogels and their composite insulation materials, using the transient plane source method to measure thermal conductivity within the temperature range of 300 to 970 K and pressure conditions from 0.045 Pa to atmospheric pressure[7]. Hua Liu, Xinlin Xia, and their team studied the transient thermal behavior of silica aerogel composites across a range of gas pressures (0.01 Pa to 100 kPa) and temperatures between 290-1090 K[8]. Ok-Joo Lee, Kun-Hong Lee, and colleagues explored the relationship between pore size and thermal conductivity in aerogels, synthesizing polyisocyanurate aerogels and measuring their thermal conductivity under conditions ranging from vacuum to ambient pressure using the transient hot-wire technique[9]. X. Lu, R. Caps, and colleagues examined the correlation between aerogel structure and thermal conductivity, measuring the thermal conductivity of both bulk and powdered aerogels[10].

Steady-state measurements, while more time-consuming, offer superior accuracy. Research has demonstrated that the steady-state method is considered the most reliable approach for determining the thermal conductivity of super-insulating materials[11]. Zhao-hui Liu, Yi-dong Ding, and co-workers Synthesized a mortar incorporating silica aerogel particles, with a focus on evaluating how the addition of fibers, air-entraining agents, and powders affects the thermal conductivity[12]. The thermal conductivity of the SiO2 aerogel mortar was measured using a flat-plate thermal conductivity instrument. Masanao Obori, Donguk Suh, and colleagues investigated the effective thermal conductivity of cellulose-nanofibril aerogels under both atmospheric and vacuum conditions, with measurements taken using a steady-state apparatus[13]. M. Glória Gomes, I. Flores-Colen, and colleagues utilized the heat flow meter method to measure the effective thermal conductivity of insulating mortars containing expanded polystyrene (EPS) and silica aerogels in hardened (28-day), dry, and varying moisture content conditions[14]. The effective thermal conductivity values obtained through the steady-state method are widely applicable in engineering.In this study, the steady-state method was employed to measure thermal conductivity, ensuring uniform heat flux through the sample. This approach determines the sample's overall thermal conductivity by applying a controlled temperature gradient. It provides the equivalent thermal conductivity, integrating conduction, convection, and radiation effects, making it particularly suitable for low thermal conductivity materials.

Distinguishing types of thermal conductivity, especially in testing refractory insulation materials, largely depends on the temperature difference. Based on test conditions, thermal conductivity can be classified into two types: true thermal conductivity and effective thermal conductivity.True thermal conductivity, which is measured under small or negligible temperature differences, reflects the inherent thermal performance of the material, while effective thermal conductivity, measured under large temperature differences, is influenced by the test environment, particularly the temperature gradient across the sample.According to ASTM standards, a small temperature difference is defined as not exceeding 25°C, while a large temperature difference is greater than 50°C. Thus, thermal conductivity measured with a temperature difference greater than 50°C is classified as effective thermal conductivity.

With the advancement of material technology, a variety of high-performance materials are being integrated into thermal insulation solutions in industrial design[15]. This study aims to examine the nonlinear variation in thermal conductivity of high-temperature insulating materials and propose a measurement and prediction method that reduces computational and time costs in industrial use. The effective thermal conductivity, measured under specific test conditions, reflects the material's performance and is affected by factors such as the temperature gradient across the sample.

In contrast, true thermal conductivity is derived from mathematical models based on experimental data. It is defined by the thermal properties of the material at a particular temperature; however, variations in measurement techniques and conditions may yield different results. To ensure accuracy and comparability, effective thermal conductivity is measured within a specified temperature range following international standards. These standards offer detailed guidelines on experimental setup, sample preparation, temperature control, and data analysis to ensure precise and consistent results.

Effective thermal conductivity values from our experiments, when combined with appropriate models, can be used to calculate the true thermal conductivity over a broader range of conditions[16]. This true thermal conductivity is critical for simulations and predictions in engineering design, ensuring that the thermal performance of materials meets the required specifications under varying operational conditions.

2. Experimental Preparation

2.1. Measurement Instruments and Test Specimens

Fig. 1 shows that the DRS-3A can measure thermal conductivity in the range of 0.0010 to 3 $Wm^{-1}K^{-1}$ with an accuracy of ±5%. For cooling, the cold side uses a semiconductor refrigeration system combined with external circulating water cooling, while the hot side is heated with an electric furnace capable of reaching temperatures up to 1200°C. The heat generated on the hot side of the semiconductor cooling plate is removed by a constant temperature water bath, specifically the HX-08 model (shown in Fig. 2), which maintains a temperature range of 0-100°C with an accuracy of ±0.05°C. The water bath has a capacity of 8 liters and a circulation pump flow rate of 13 L/min. During the experiment, the flow rate of the cooling water between the thermal conductivity tester and the low-temperature constant temperature water bath is controlled using a flow meter.

Fig. 1 DRS-3A High-temperature thermal conductivity tester

Fig. 2 Low-temperature constant temperature water tank

In contemporary applications, high-temperature insulation materials are predominantly classified into two categories: fibrous insulation materials and aerogel-based materials. Fibrous insulation materials comprise asbestos and its derivatives, rock wool and its derivatives, and aluminum silicate refractory fibers and their derivatives. Specifically, for environments where temperatures exceed 500°C, aluminum silicate needled felts, high-dimensional S blankets, and nano-aerogel blankets are extensively employed as effective high-temperature insulation solutions.This study uses three different types of high-temperature insulation cotton materials. The dimensions of each sample are 250 mm in length, 250 mm in width, and 50 mm in thickness. Fig. 3 shows the actual samples of the high-dimensional S blanket, aluminum silicate cotton needle felt, and nano-aerogel blanket.

High-dimensional S blanket

Aluminum silicate cotton needle felt

Nano-aerogel blanket

Fig. 3 Test piece

2.2. Measuring principle

The DRS-3A thermal conductivity tester uses the heat flow meter method and complies with ASTM C518[17] standards, as shown in Fig. 4. In the schematic, U' is the cooling unit, U" the heating unit, H the heat flow meter, and S the sample.

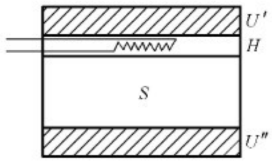

Fig. 4 DRS-3A Internal Basic Structure

The effective thermal conductivity is calculated using the formula:

$$\lambda_{Eff} = \frac{q''*L}{T_H - T_C} \tag{1}$$

Where λ_{Eff} is effective thermal conductivity, q'' is heat flux, L is sample thickness. T_H is hot-side average temperature and T_C is cold-side average temperature.

For insulating materials of a certain thickness, the relationship between effective thermal conductivity and true thermal conductivity is given by:

$$\lambda_{Eff}(T_H, T_C) = \frac{1}{T_H - T_C} \int_{T_C}^{T_H} \lambda_{True}(T)\, dT \tag{2}$$

Where λ_{Ture} is ture thermal conductivity, and T is temperature.

If thermal conductivity is a linear function of temperature, then the effective thermal conductivity is the conductivity at the average temperature $\bar{T}$= $(T_H+T_C)/2$. However, for materials with highly nonlinear thermal conductivity, the effective thermal conductivity must be combined with a physical model to provide valuable data.

Assuming that the effective thermal conductivity λ_{Eff} can be represented as a cubic function of the average temperature as given by Eq. (3), the coefficients A_0, A_1, A_2, and A_3 are determined via least squares fitting of the experimental data, resulting in the relationship:

$$\lambda_{Eff}(\bar{T}) = A_0 + A_1\bar{T} + A_2\bar{T}^2 + A_3\bar{T}^3 \tag{3}$$

Where $\bar{T}$ is the arithmetic average of the cold-side and hot-side temperatures.

Assuming that the true thermal conductivity of the sample varies with temperature as a cubic polynomial:

$$\lambda_{True}(\bar{T}) = B_0 + B_1\bar{T} + B_2\bar{T}^2 + B_3\bar{T}^3 \tag{4}$$

Where B_0, B_1, B_2, and B_3 are undetermined constants intrinsic to the material. By employing Eq. (2), the relationship between the effective thermal conductivity λ_{Eff} and the temperatures at the cold side T_C and hot side T_H of the sample is derived, as described by Eq. (5):

$$\lambda_{Eff,Cal} = B_0 + B_1\frac{(T_H+T_C)}{2} + B_2\frac{(T_H{}^2+T_HT_C+T_C{}^2)}{3} + B_3\frac{(T_H{}^2+T_C{}^2)(T_H+T_C)}{4} \tag{5}$$

Where $\lambda_{Eff,Cal}$ is clculated effective thermal conductivity.

By substituting the experimental data namely, the effective thermal conductivity λ_{Eff}, and the temperatures T_C and T_H of the sample's cold and hot sides into Eq. (5), the coefficients B_0, $B1$, $B2$, and B_3 can be determined. This allows for the ascertainment of the true thermal conductivity, as described by Eq. (4).

To verify the accuracy and deviation of the expression for the true thermal conductivity λ_{Eff}, the experimental temperatures T_H and T_C, along with the determined coefficients B_0, B_1, B_2, and B_3, are substituted back into Eq. (5) to obtain the theoretically predicted effective thermal conductivity $\lambda_{Eff,Cal}$. The error is then computed by comparing the predicted $\lambda_{Eff,Cal}$ with the experimentally measured λ_{Eff}, as given by Eq. (6)：

$$error = \frac{|\lambda_{Eff,Exp} - \lambda_{Eff,Cal}|}{\lambda_{Eff,Exp}} * 100\% \tag{6}$$

Where $\lambda_{Eff,Exp}$ is experimental effective thermal conductivity.

The precision of the measurement tools, such as the temperature sensors, sample thickness measuring tools, and heat flux meter, is one of the main sources of uncertainty. Examining these instruments' calibration data allows one to determine the systematic and random mistakes. The process of fitting the data also creates uncertainty; in the least squares fitting approach, the accuracy of the fitting is assessed by computing the standard errors of the fitting coefficients. The expected error margin is roughly ±5%, based on data fitting analyses and several experiments.

3. Experimental results and analysis

This study investigates the thermal conductivity of three insulating materials, examining the effects of various temperature conditions and relative humidity levels on their thermal properties. A total of 90 experimental were established conditions involving three types of insulating materials: high-dimensional S blanket, aluminum silicate cotton needle felt, and nano-aerogel blanket. The experimental conditions are categorized into two environmental scenarios: ambient temperature with drying and 60% relative humidity. Thermal conductivity was measured at 15 discrete temperature points for each scenario. Each dataset includes the nominal temperature (T_N), cold-side temperature, hot-side temperature, and effective thermal conductivity of the sample. For each condition, the mean values of the cold-side temperature, hot-side temperature, and effective thermal conductivity were computed from 10 individual measurements. Tab. 1 presents the temperature data for the nano-aerogel blanket under dry conditions. These mean values are designated as the cold-side temperature (T_C), hot-side temperature (T_H), and effective thermal conductivity (λ_{Eff}) for each experimental condition. The mean temperature is then calculated as the arithmetic average of the cold-side and hot-side temperatures, represented by $\bar{T}=(T_H+T_C)/2$.

Tab. 1，The temperature experimental data for the nano-aerogel blanket under dry conditions

T_N / °C	T_H / °C	T_C / °C	T_N / °C	T_H / °C	T_C / °C
50	52.55	20.37	450	452.87	20.31
100	97.13	20.85	500	503.52	29.33
150	146.59	20.69	550	548.94	33.94
200	202.55	20.14	600	604.67	308.29
250	251.21	21.59	625	625.64	350.11
300	300.68	20.40	650	650.64	368.92
350	350.35	21.54	700	703.38	445.16
400	401.11	20.89			

The experimental data for high-dimensional S blanket, aluminum silicate cotton needle felt, and nano-aerogel blanket under dry and 60% humidity conditions were fitted using individual curve fitting, covering ninety separate experimental scenarios. The resulting equations, derived based on Eq. (3), describe the relationship between effective thermal conductivity and average temperature for both humidity conditions.

High-dimensional S blanket.

Dry conditions:

$$\lambda_{Eff}(\bar{T}) = 1.4831E-01-1.1236E-04\bar{T}+3.7829E-06\bar{T}^2-4.2817E-09\bar{T}^3 \quad (7)$$

60% relative humidity:

$$\lambda_{Eff}(\bar{T}) = 1.6538E-01-3.9719E-04\bar{T}+5.4282E-06\bar{T}^2-6.1978E-09\bar{T}^3 \quad (8)$$

Aluminum silicate cotton needle felt.

Dry conditions:

$$\lambda_{Eff}(\overline{T}) = 1.7854E-01 - 3.3281E-04\overline{T} + 4.5664E-06\overline{T}^2 - 5.2553E-09\overline{T}^3 \quad (9)$$

60% relative humidity:

$$\lambda_{Eff}(\overline{T}) = 1.6657E-01 - 2.9174E-05\overline{T} + 3.4410E-06\overline{T}^2 - 4.3676E-09\overline{T}^3 \quad (10)$$

Nano-aerogel blanket.

Dry conditions:

$$\lambda_{Eff}(\overline{T}) = 1.3963E-01 - 6.2694E-04\overline{T} + 3.9603E-06\overline{T}^2 - 3.7393E-09\overline{T}^3 \quad (11)$$

60% relative humidity:

$$\lambda_{Eff}(\overline{T}) = 1.3472E-01 - 6.4302E-04\overline{T} + 4.3573E-06\overline{T}^2 - 4.3651E-09\overline{T}^3 \quad (12)$$

Fig. 5, Fig. 6, and Fig. 7 present the fitted curves for the three types of insulating materials under dry and 60% humidity conditions, illustrating the fluctuation of effective thermal conductivity with average temperature.

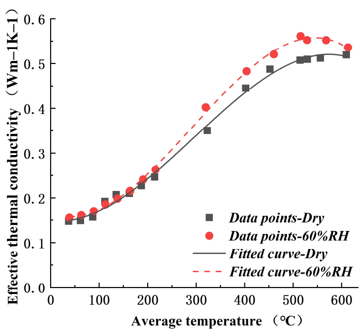

Fig 5 The variation of the effective thermal conductivity of the high-dimensional S blanket as a function of average temperature.

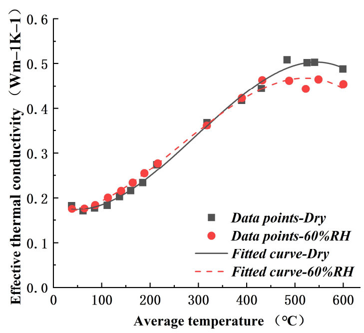

Fig 6 The variation of the effective thermal conductivity of the aluminum silicate cotton needle felt as a function of average temperature.

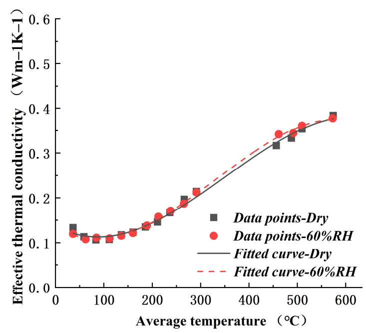

Fig 7 The variation of the effective thermal conductivity of the nano-aerogel blanket as a function of average temperature.

3.1. Effective thermal conductivity of high-dimensional S blanket under different temperature and humidity conditions.

According to Fig. 5, under dry conditions, effective thermal conductivity(λ_{Eff}) increases with rising average temperature at temperatures below 500°C. Around 550°C, λ_{Eff} increases more slightly and then exhibits a downward trend. At approximately 700°C, λ_{Eff} reaches its maximum value, 0.5193.

Under 60% humidity conditions, λ_{Eff} increases with average temperature when it is below 500°C. Beyond 550°C, λ_{Eff} starts to decrease. At approximately 600°C, λ_{Eff} reaches its peak value, approximately 0.5613.

Fig. 5 illustrates that at average temperatures below 86.86℃, the effective thermal conductivity under dry conditions exceeds that under 60% humidity. Within the temperature range of 86.86℃ to 613.24℃, the effective thermal conductivity under dry conditions is lower than that under 60% humidity. The influence of humidity on the thermal conductivity of this material becomes more significant as the temperature exceeds 200℃.

3.2. Effective thermal conductivity of aluminum silicate cotton needle felt under different temperature and humidity conditions.

According to Fig. 6, under dry conditions, the effective thermal conductivity λ_{Eff} decreases with rising average temperature when the average temperature is below 100°C. Between 100°C and 500°C, λ_{Eff} increases with temperature. Beyond 550°C, λ_{Eff} decreases with further temperature increase. The effective thermal conductivity λ_{Eff} reaches its minimum value, approximately 0.1707, around 100°C and its maximum value, approximately 0.5081, around 600°C.

Under 60% humidity conditions, λ_{Eff} increases with average temperature when it is below 500°C. Around 550°C, λ_{Eff} decreases as the temperature continues to rise, reaching its peak value, approximately 0.5613, around 550°C.

Fig. 6 demonstrates that when the average temperature is below 390 ℃, the effective thermal conductivity under dry conditions is slightly less than that under 60% humidity. However, when the temperature exceeds 389.74℃, the thermal conductivity under dry conditions becomes greater than that under 60% humidity, indicating a more pronounced impact of humidity at elevated temperatures.

3.3. Effective thermal conductivity of nano-aerogel blanket under different temperature and humidity conditions

According to Fig. 7, under dry conditions, the effective thermal conductivity λ_{Eff} decreases with rising average temperature when the average temperature is below 150°C. Between 150°C and 600°C, λ_{Eff} increases with temperature. The effective thermal conductivity λ_{Eff} reaches its minimum value, approximately 0.1060, around 150°C.

Under 60% humidity conditions, λ_{Eff} decreases with average temperature when it is below 100°C. Between 100°C and 600°C, λ_{Eff} increases with temperature. The effective thermal conductivity λ_{Eff} reaches its minimum value, approximately 0.1077, around 100°C.

Fig. 7 suggests that at average temperatures below 291℃, the effective thermal conductivity under dry conditions closely matches that under 60% humidity. As the temperature rises above 291℃, the conductivity under dry conditions becomes slightly lower than that at 60% humidity. Overall, the effect of humidity on the thermal conductivity of this material remains insignificant up to temperatures of 600℃.

In least squares fitting, the accuracy of coefficients B_0, B_1, B_2, and B_3 depends on experimental data precision, where even slight noise can cause significant deviations. This research employs a cubic polynomial to model the thermal conductivity-temperature relationship, yet real materials often display more complex nonlinear behavior, potentially introducing systematic errors, especially at temperature extremes. Errors may arise from inaccuracies in heat flux and temperature measurements, as well as uncertainties in sample thickness, all of which can affect the reliability of the fitting results.

4. Prediction of true thermal conductivity and effective thermal conductivity

The thermal conductivity data for fifteen different conditions in dry and 60% humidity environments were analyzed. For each condition, data from eight specific nominal temperature points (50°C, 150°C, 250°C, 350°C, 450°C, 550°C, 625°C, and 700°C) were selected and fitted using the least squares method. These fittings were expressed in the form of Eq. (5), yielding the undetermined coefficients B_0, B_1, B_2, and B_3. By substituting B_0, B_1, B_2, and B_3 into Eq. (4), the true thermal conductivity of the sample under both dry and 60% humidity conditions was determined.

High-dimensional S blanket

Dry conditions:

$$\lambda_{True}(\bar{T}) = 1.5452E-01 - 3.3223E-04\bar{T} + 4.5849E-06\bar{T}^2 - 4.9675E-09\bar{T}^3 \quad (13)$$

60% relative humidity:

$$\lambda_{True}(\bar{T}) = 1.6320E-01 - 4.8907E-04\bar{T} + 5.8045E-06\bar{T}^2 - 6.4845E-09\bar{T}^3 \quad (14)$$

Aluminum silicate cotton needle felt.

Dry conditions:

$$\lambda_{True}(\bar{T}) = 1.9842E-01 - 7.5918E-04\bar{T} + 5.9642E-06\bar{T}^2 - 6.4192E-09\bar{T}^3 \quad (15)$$

60% relative humidity:

$$\lambda_{True}(\bar{T}) = 1.7231E-01 - 2.0186E-04\bar{T} + 4.1005E-06\bar{T}^2 - 4.9511E-09\bar{T}^3 \quad (16)$$

Nano-aerogel blanket.

Dry conditions:

$$\lambda_{True}(\bar{T}) = 1.6357E-01 - 1.0958E-03\bar{T} + 5.2830E-06\bar{T}^2 - 4.6408E-09\bar{T}^3 \quad (17)$$

60% relative humidity:

$$\lambda_{True}(\bar{T}) = 1.5064E-01 - 1.0050E-03\bar{T} + 5.2818E-06\bar{T}^2 - 4.8422E-09\bar{T}^3 \quad (18)$$

Fig. 8 display the fitted curves for three distinct types of insulating materials at dry and 60% humidity, illustrating the variation in true thermal conductivity as a function of average temperature.

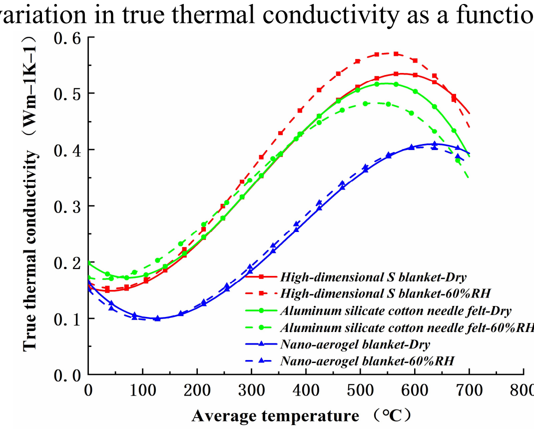

Fig 8 The variation of the true thermal conductivity of high-temperature resistant porous insulations as a function of average temperature

By substituting the fitted coefficients B_0, B_1, B_2, and B_3 into Eq. (5), the prediction equation for the effective thermal conductivity (λ_{Eff}) under dry and 60% humidity conditions was derived. The remaining data points (100°C, 200°C, 300°C, 400°C, 500°C, 600°C, 650°C) were then used in Eq. (6) to calculate the theoretical effective thermal conductivity ($\lambda_{Eff,Cal}$). The error between the theoretical ($\lambda_{Eff,Cal}$) and experimentally measured (λ_{Eff}) values was analyzed. Tab.2, Tab. 3, and Tab. 4 present the effective thermal conductivity (λ_{Eff}), the theoretically predicted values ($\lambda_{Eff,Cal}$), and the calculation errors for the three types of samples under both conditions.

Tab. 2 Experimental and calculated effective thermal conductivity of high-dimensional S blanket, along with their respective errors.

T_N / °C	$\lambda_{Eff,Exp}$	$\lambda_{Eff,Cal}$	*error*	$\lambda_{Eff,Exp(60\%)}$	$\lambda_{Eff,Cal(60\%)}$	*error* $_{(60\%)}$
100	0.1491	0.1522	2.10%	0.1612	0.1561	3.18%
200	0.1921	0.1752	8.80%	0.1857	0.1817	2.14%
300	0.2099	0.2138	1.84%	0.2158	0.2268	5.10%
400	0.2462	0.2613	6.14%	0.2631	0.2820	7.18%
500	0.4452	0.4351	2.27%	0.4831	0.4786	0.92%
600	0.5074	0.5123	0.96%	0.5613	0.5544	1.24%

650	0.5121	0.5219	1.91%	0.5524	0.5571	0.85%

As shown in Tab. 2, for the high-dimensional S blanket under ambient dry conditions, the calculation errors range from 0.96% to 8.80%, with the maximum error observed at 200°C and the minimum error at 600°C. Under 60% humidity conditions, the errors range from 0.85% to 7.18%, with the maximum error at 400°C and the minimum error at 650°C.The discrepancy between the experimental and calculated values diminishes at higher temperatures (above 500°C), indicating that the calculation model is more accurate for this material at high temperatures in both environments.

Tab. 3 Experimental and calculated effective thermal conductivity of aluminum silicate cotton needle felt, along with their respective errors.

T_N / °C	$\lambda_{Eff,Exp}$	$\lambda_{Eff,Cal}$	*error*	$\lambda_{Eff,Exp(60\%)}$	$\lambda_{Eff,Cal(60\%)}$	*error* $_{(60\%)}$
100	0.1707	0.1754	2.72%	0.1762	0.1767	0.26%
200	0.1835	0.1890	3.02%	0.2005	0.2008	0.15%
300	0.2162	0.2215	2.45%	0.2338	0.2387	2.09%
400	0.2743	0.2674	2.51%	0.2771	0.2810	1.39%
500	0.4174	0.4220	1.09%	0.4230	0.4183	1.10%
600	0.5081	0.4871	4.13%	0.4617	0.4637	0.44%
650	0.5025	0.5016	0.17%	0.4646	0.4659	0.28%

As shown in Tab.3, for aluminum silicate cotton needle felt under ambient dry conditions, the calculation errors range from 0.17% to 4.13%, with the maximum error at 600°C and the minimum error at 650°C. Under 60% humidity, the errors range from 0.28% to 2.09%, with the maximum error at 300°C and the minimum error at 650°C.Higher temperatures (above 500°C) in a 60% humidity environment, the errors between the experimental and calculated values decrease, indicating higher accuracy of the calculation model.

Tab. 4 Experimental and calculated effective thermal conductivity of nano-aerogel blanket, along with their respective errors.

T_N / °C	$\lambda_{Eff,Exp}$	$\lambda_{Eff,Cal}$	*error*	$\lambda_{Eff,Exp(60\%)}$	$\lambda_{Eff,Cal(60\%)}$	*error* $_{(60\%)}$
100	0.1131	0.1185	4.79%	0.1077	0.1107	2.79%
200	0.1069	0.1110	3.83%	0.1099	0.1089	0.89%
300	0.1232	0.1246	1.10%	0.1217	0.1256	3.19%
400	0.1458	0.1522	4.40%	0.1579	0.1557	1.37%
500	0.1968	0.1883	4.30%	0.1870	0.1927	3.03%
600	0.3164	0.3149	0.47%	0.3418	0.3239	5.23%
650	0.3537	0.3510	0.75%	0.3614	0.3530	2.31%

As shown in Tab. 4 ， for nano-aerogel blanket under ambient dry conditions, the calculation errors range from 0.47% to 4.79%, with the maximum error at 100°C and the minimum error at 600°C. Under 60% humidity, the errors range from 0.89% to 5.23%, with the maximum error at 600°C and the minimum error at 200°C. At higher temperatures (above 500°C) in ambient dry conditions, the errors between experimental and calculated values decrease, indicating higher accuracy of the calculation model.

Tab. 2, Tab. 3, and Tab. 4 show that for these three porous materials under both dry and 60% humidity conditions, the errors between the calculated effective thermal conductivity and the experimentally measured effective thermal conductivity do not exceed 8.80%. The fitting results are excellent, effectively predicting the effective thermal conductivity of these three porous materials within the experimental temperature range, demonstrating the reliability of this method.

The observed deviations stem from several sources: data fluctuations at certain temperatures, limitations of the fitting model, changes in thermal conduction at high temperatures, and reduced measurement accuracy at low temperatures. These factors collectively introduce uncertainties in the results.

5. Conclusion

The effective thermal conductivity of three insulation materials high-dimensional S blanket, aluminum silicate needle felt, and nano-aerogel blanket was experimentally measured at various temperatures and two humidity levels. Using the least squares method, the relationship between effective thermal conductivity and average temperature was derived from the experimental data.

Based on the derived relationship, the true thermal conductivity was determined as a function of the average temperature for these materials. By employing the true thermal conductivity, the effective thermal conductivity was predicted under 42 different experimental conditions. For the dry samples, the maximum error between predicted and experimentally measured effective thermal conductivity was 8.80%, while for the sample at 60% humidity, the maximum error was 7.18%. Despite inherent errors, the fitting model's predictive accuracy generally meets engineering application requirements across diverse conditions, showcasing its robustness and practical utility in real-world scenarios.

The results demonstrate that humidity significantly influences both the effective and true thermal conductivity of materials at high temperatures. However, for nano-aerogel insulation materials, the impact of humidity on thermal conductivity is negligible below 600°C.

This study's experimental and computational findings on thermal conductivity offer valuable insights for designing thermal protection in aerospace and engine thermal management.

Nomenclature

λ_{Eff}	Effective thermal conductivity	$Wm^{-1}K^{-1}$
$\lambda_{Eff,Exp}$	Experimental effective thermal conductivity	$Wm^{-1}K^{-1}$
$\lambda_{Eff,Cal}$	Calculated effective thermal conductivity	$Wm^{-1}K^{-1}$
λ_{True}	Ture thermal conductivity	$Wm^{-1}K^{-1}$
T	Temperature	℃
T_N	Nominal temperature	℃
T_H	Hot-side average temperature	℃
T_C	Cold-side average temperature	℃
$\bar{T}$	The arithmetic average of the cold-side and hot-side temperatures	℃
q''	Heat flux	$W \cdot m^{-2}$
L	Sample thickness	m

References

[1] Zhang, L.B., et al., Tungsten-rhenium thermocouple sensor for in-situ ultra-high temperature measurement of hypersonic aircraft surface, *Proceedings*, IET & ISA 60th International Instrumentation Symposium 2014, June 2014, pp. 1-5

[2] Uyanna, O., Najafi, H., Thermal Protection Systems For Space Vehicles: A Review On Technology Development, Current Challenges And Future Prospects, *Acta Astronautica*, *176* (2020), pp. 341-356

[3] Hrubesh, L.W., Pekala, R.W., Thermal Properties Of Organic And Inorganic Aerogels, *Journal of Materials Research*, *9* (1994), 3, pp. 731-738

[4] Daryabeigi, K., Heat Transfer In High-Temperature Fibrous Insulation, *Journal of Thermophysics and Heat Transfer*, *17* (2003), 1, pp. 10-20

[5] Stark, C., Fricke, J., Improved Heat-Transfer Models For Fibrous Insulations, *International Journal of Heat and Mass Transfer*, *36* (1993), 3, pp. 617-625

[6] Verschoor, J.D., Greebler, P., Heat Transfer By Gas Conduction And Radiation In Fibrous Insulations, *Journal of Fluids Engineering*, *74* (1952), 6, pp. 961-967

[7] Wei, G., et al., Thermal Conductivities Study On Silica Aerogel And Its Composite Insulation Materials, *International Journal of Heat and Mass Transfer*, *54* (2011), 11, pp. 2355-2366

[8] Liu, H., et al., Experiment And Identification Of Thermal Conductivity And Extinction Coefficient Of Silica Aerogel Composite, *International Journal of Thermal Sciences*, *121* (2017), pp. 192-203

[9] Lee, O.-J., et al., Determination Of Mesopore Size Of Aerogels From Thermal Conductivity Measurements, *Journal of Non-Crystalline Solids*, *298* (2002), 2, pp. 287-292

[10] Lu, X., et al., Correlation Between Structure And Thermal Conductivity Of Organic Aerogels, *Journal of Non-Crystalline Solids*, *188* (1995), 3, pp. 226-234

[11] Merillas, B., et al., Thermal Conductivity Of Nanoporous Materials: Where Is The Limit?, *Polymers*, *14* (2022), 13, pp. 2556

[12] Liu, Z., et al., Thermal Insulation Material Based On SiO2 Aerogel, *Construction and Building Materials*, *122* (2016), pp. 548-555

[13] Obori, M., et al., Parametric Model To Analyze The Components Of The Thermal Conductivity Of A Cellulose-Nanofibril Aerogel, *Phys. Rev. Appl.*, *11* (2019), 2, pp. 024044

[14] Gomes, M.G., et al., Thermal Conductivity Measurement Of Thermal Insulating Mortars With EPS And Silica Aerogel By Steady-State And Transient Methods, *Construction and Building Materials*, *172* (2018), pp. 696-705

[15] Zhang, Z., et al., Effect Of Inlet Conditions On The Thermal Insulation Performance Of Marine Gas Turbine Exhaust Systems, *Thermal Science*, (2024), 00, pp. 160-160

[16] Qian, W., et al., Physics-Informed Neural Network For Inverse Heat Conduction Problem, *Heat Transf. Res.*, *54* (2023), 4, pp. 65-76

[17] Materials, A., Designation C518-91: Standard Test Method For Steady-State Heat Flux Measurements And Thermal Transmission Properties By Means Of The Heat FlowMeter Apparatus, *Annual Book of ASTM Standards*, *04* (1985), pp. 151-162

Received: 18.11.2024.
Revised: 2.3.2025.
Accepted: 25.3.2025.